Journal of Engineering Physics and Thermophysics, Vol. 77, No. 2, 2004

DRAG AND ROTATIONAL PROPERTIES OF CASCADES OF CIRCULAR CYLINDERS AT SMALL AND MODERATE REYNOLDS NUMBERS

A. B. Mazo and I. V. Morenko

UDC 532.516

An iteration method of calculating pressure by solving Navier–Stokes equations in stream function–vortex variables is proposed. A numerical investigation of the drag and the rotational properties of cascades of circular cylinders at small and moderate Reynolds numbers has been carried out.

Introduction. In investigating a flow around a blade cascade it is important to know the dependence of the drag and the rotational properties of the cascade on its spacing, the velocity of the flow, and the angle of its incidence. The problem was solved for a particular case of high flow velocities where the parameters of the flow depend only slightly on the Reynolds number [1–3]. For example, the rotational properties of cascades in the case where a gas flow is incident on them at an angle close to $\pi/2$ have been experimentally investigated in [3]. In this case, the refractive index of a cascade of a round wire is determined as

$$\alpha = \tan \alpha^{+} / \tan \alpha^{-} . \tag{1}$$

It has been established empirically that the dependence of the refractive index of such a cascade on its drag C has the form $\alpha = 1/\sqrt{1+C}$.

The present work is devoted to theoretical investigation of the drag and the rotational properties of a cascade at moderate Reynolds numbers $\mathrm{Re} > 1$ at which both the inertial and the viscous forces are significant and a stationary laminar vortex wake is formed downstream of each of the circular cylinders composing the cascade. This regime of flow is characterized by the fact that the main hydrodynamic parameters depend substantially on Re. Various formulations of the boundary-value problems for Navier–Stokes equations in stream function ψ–vorticity ω variables were used in the calculations.

Calculation of the Cascade Drag. In calculating the drag coefficient C we separated a periodicity cell — a tube of flow of width H — and numerically solved the problem on a steady symmetric flow around an individual cylinder of unit radius, at the boundary streamlines of which $y = \pm H/2$ the ideal slipping conditions were set. It was assumed that at a large distance from the obstacle ($x \to \pm\infty$) the flow is uniform, $\psi = y$ and $\omega = 0$. In this case, the boundary of the streamlined cylinder Γ is a zero streamline $\psi = 0$ at which the adhesion conditions $\partial\psi/\partial n = 0$ are additionally set.

The stationary fields of ψ and ω are determined by solving the evolution problem with the use of algorithms traditional for equations of this type [4, 5]. At each time step, the vorticity-transfer equation and the Poisson equation for the stream function are solved successively, and the nonlinear convective terms in the equation for ω are taken from the previous time layer. Approximation of the Navier–Stokes equations and calculations are performed by the first-order finite-element method (FEM) on irregular grids bunching to the contour Γ [6]. The enumeration of the FEM-grid nodes is optimized with the use of a minimum-power algorithm, which provides a band structure of the matrices of the FEM linear systems and minimizes the calculations necessary for their inversion by the Kholetskii method. Since the desired functions change significantly only in the neighborhood of a streamlined body, the use of FEM grids that are fine in this region and coarse outside it plays a crucial role in decreasing the calculations. A testing of the algorithm on a series of bunching grids has shown that a fairly accurate solution of the problem can be

Institute of Mechanics and Machine Manufacturing, Kazan' Research Center, Russian Academy of Sciences, 2/31 Lobachevskii Str., Kazan', 420111, Russia; email: amazo@ksu.ru, morenko@mail.knc.ru. Translated from Inzhenerno-Fizicheskii Zhurnal, Vol. 77, No. 2, pp. 75–79, March–April, 2004. Original article submitted August 8, 2003.

1062-0125/04/7702-0338

obtained even on a grid of 6500 triangles with a ratio between the areas of the large and small elements of the order of 100. At Re = 30 and a time step $\tau = 0.05$, a stationary solution is obtained in 910 steps ($t = 45.5$) and the time of calculations on an Athlon-1700 computer is 17 sec.

The pressure is calculated by the known equation [4]

$$\Delta p = f(x, y) \equiv 2\left[\frac{\partial^2\psi}{\partial x^2}\frac{\partial^2\psi}{\partial y^2} - \left(\frac{\partial^2\psi}{\partial x \partial y}\right)^2\right]. \tag{2}$$

The Neumann condition $\partial p/\partial n = 0$ is set at all the outer boundaries of the computational region D and the Pirson condition is set at the boundary of the streamlined cylinder [4]:

$$x, y \in \Gamma: \ \frac{\partial p}{\partial n} = \frac{1}{\mathrm{Re}}\frac{\partial \omega}{\partial s}. \tag{3}$$

The difficulties associated with the numerical solution of problem (2)–(3) are described in a number of works [4, 7, 8]. For example, Roache [4] points to the degeneracy of this problem and proposes a condition at which it can be overcome. This condition is not fulfilled exactly in the calculations; therefore, the right-hand side of Eq. (2) is replaced by

$$\bar{f} = f - \langle f \rangle, \quad \langle f \rangle = \frac{1}{|D|}\int_D f\, dx dy = 0, \tag{4}$$

and, to obtain a unique solution, it is recommended to set the Dirichlet condition at a part of the boundary; for example, $p = p_1 = 0$ as $x \to -\infty$.

However, this technique does provide a stable solution, which becomes most evident in the case where the pressure of a cascade with a small spacing is calculated. This is explained by three complicating circumstances:

(1) the low accuracy of the determination of the right side f of Eq. (2) expressed in terms of the second derivatives of an approximate grid solution with respect to ψ;

(2) the large elongation of the D region (in the calculations, the boundaries positioned at an infinite distance from the obstacle $x = \pm\infty$ are replaced by the finite boundaries $x = \pm L$, $|L| >> 1$);

(3) the structure of the right side of the constitutive equation (f in formulation (4) differs from zero only in the neighborhood of the streamlined body, whose dimension is comparable to the length of the vortex wake).

The first two circumstances are responsible for the errors in the calculation of the pressure. It is easy to show that the error ε in f can lead to an error of the order of εL^2 in p. To decrease ε at the stage of calculation of the pressure, it is necessary to refine the stream function ψ by solving the problem $-\Delta\psi = \omega$ over again with the use of third-power finite elements. This makes it possible to determine the right side f of Eq. (2) with sufficient accuracy.

Because of circumstance (3) and the Neumann boundary conditions, the desired solution has the following structure. The pressure changes substantially only in the above-mentioned neighborhood of the body and is constant outside it. In this case, the pressure difference $p_1 - p_2 = -p_2 = p(L)$ determines the drag coefficient of the cascade $C = -p_2$. On the other hand, the coefficient C can be calculated by integrating the viscous and pressure forces over the streamlined contour [5]:

$$C = (C_f + C_p)/H = \int_\Gamma [\mathrm{Re}^{-1}\,\omega \cos(\hat{s}, \hat{x}) + p \sin(\hat{s}, \hat{x})]\, ds/H. \tag{5}$$

This allows one to construct an iteration algorithm that would make it possible to obtain a stable solution of Eq. (2). As the initial approximation, a solution of problem (2)–(3) with the Neumann condition in the cross section $x = L$ serves. In the subsequent iterations, formula (5) for the drag coefficient C, by which the pressure p_2 is refined at the boundary $x = L$, is used in each step and the problem with the Dirichlet conditions $p(-L) = 0$ and $p(L) = p_2$ is solved. The calculations show that three or four iterations would suffice to attain the convergence (C is determined with an accuracy of the order of 10^{-4}). An example of the calculation is presented in Fig. 1. It shows all the features of the pressure

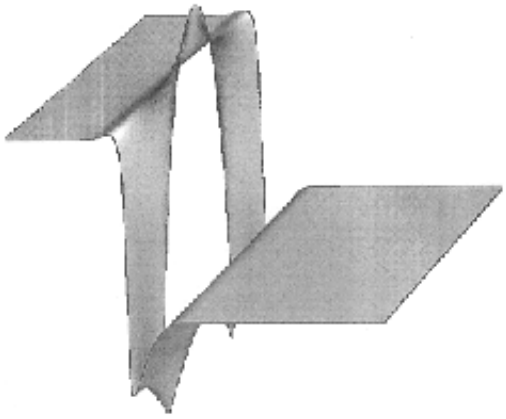

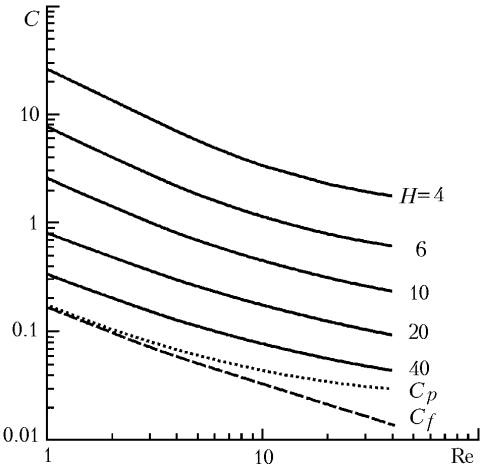

Fig. 1. Pressure distribution in the symmetric flow around a cascade with a spacing $H = 4$ at Re = 30. The figure is crimped along the x axis.

Fig. 2. Dependence of the drag coefficient of the cascade C on the Reynolds number Re and the spacing H. The dashed and dash-dot lines denote the friction drag coefficient and the pressure drag coefficient for $H = 40$.

distribution: p remains unchanged at any distance from the obstacle upstream and downstream of it, the pressure increases abruptly on the windward side of the cylinder, and the pressure is depressed at the bottom of the cylinder.

The numerical algorithm was tested for the case of an infinite flow around an individual circular cylinder considered as a limiting case of a cascade as $H \to \infty$ and in the range $1 \le \mathrm{Re} \le 40$. It has been established that the influence of the computational region boundaries on the solution becomes negligibly small at $H > 40$. In the process of testing we compared the streamlines, the constant-vorticity lines, the distribution of p and ω over the contour of the cylinder, and the dependences of the angle of flow separation, the length of the vortex region, and the drag coefficient $C_D = CH$ on the Reynolds number. As the testing data, we used the calculations of ψ and ω of different authors [9], the photographs of a separation flow [10], the pressure distribution over the contour of a streamlined body calculated by Apelt and Kavaguti and obtained experimentally by Thom [5, 7, 9], and the numerical dependences of the vortex-region length [9, 11] and the angle of flow separation on Re [5, 12]. The dependences of C_D, C_f, and C_p on Re were tested by the analytical and numerical solutions, the empirical data [11–13], and the data generalized in [5, 9]. We also used the data obtained with a universal FLUENT package. The calculated p is closest to the Kavaguti curve, and the distribution of ω over the contour of the cylinder differs from that of [5] by approximately 3% on the leeward side of the cylinder. The calculated curve $C_D(\mathrm{Re})$ passes through the upper experimental points of different authors. The other results of the numerical modeling agree well with the test data.

The results of the calculation of the cascade drag in the form of the dependences of C, C_f, and C_p on Re and H are presented in Fig. 2.

It should be noted that in the case where the Reynolds number changes in the range $1 \le \mathrm{Re} \le 4$, the flow in the cascade is unseparated. At $\mathrm{Re} \ge 5$, a pair of stationary vortices arise downstream of each of the cylinders independently of the cascade spacing. The critical Reynolds number, at which an instability begins to develop and a Kármán vortex street appears, depends on H. For example, for a cascade with a spacing of $H = 40$ (an unbounded flow) the critical Re is equal to 41, and for a cascade with a spacing of $H = 4$ the regime of flow changes at Re = 62.

Determination of the Rotational Properties of a Cascade. Despite the fact that the profile of the elements of cascades of circular cylinders is not directional, these cascades can rotate the flow [2, 3]. This is supported by the results of numerical modeling of a uniform flow of a viscous fluid incident on a cascade of 15 cylinders from the left at an angle α^- (see Fig. 3).

As the flow passes through a row of cylinders, its velocity vector rotates through an angle $\alpha^+ \le \alpha^-$ (in modeling, the angle of incidence α^- is prescribed and the angle of outflow α^+ is determined from the pattern of the cal-

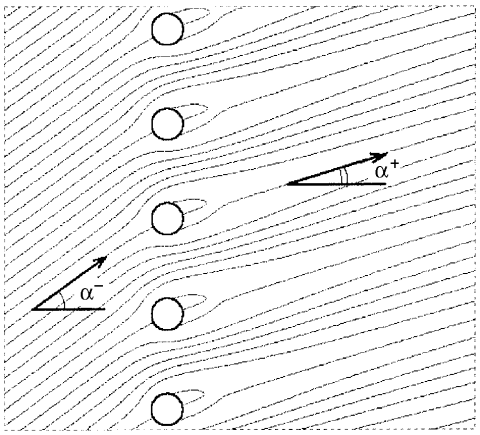

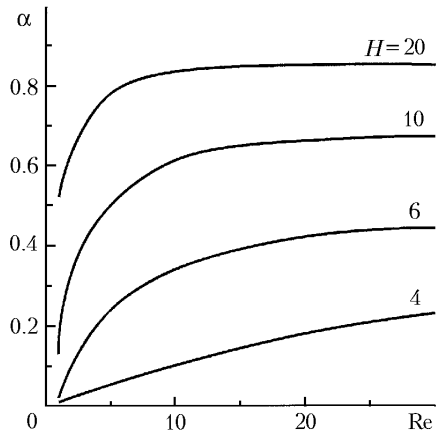

Fig. 3. Lines of the asymmetric flow around a cascade with a spacing H = 6 at Re = 20.

Fig. 4. Dependence of the refractive index of the cascade α on the Reynolds number Re and the spacing H.

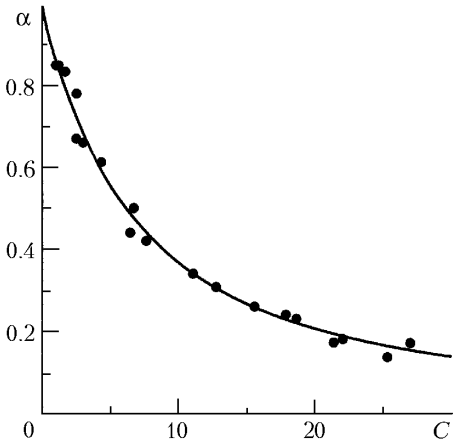

Fig. 5. Dependence of the refractive index α on the drag coefficient for a cascade of circular cylinders. Numerical experiment (points) and approximation by formula (6).

culated streamlines, as shown in Fig. 3). It is evident that at a large distance from the obstacle, downstream of it, the direction of the flow is determined by the shape of the outer boundaries of the computational region which are formed by the straight walls with angles of inclination $\beta^- = \alpha^-$ upstream of the cascade and β^+ downstream of it. However, the influence of the directions β^- and β^+ on α^+ is small, especially for the central streamlines. Therefore, the coefficient α is determined in the process of successive approximations, in each of which the angle $\beta^+ = \alpha^+$ is refined, the finite-element grid is constructed over again, and the Navier–Stokes problem is solved. The process is converged in two or three iterations. The index of refraction α is determined by formula (1).

In the course of the numerical experiment performed, by the above-described method we determined the influence of the Reynolds number Re and the cascade spacing H on the refractive index α (Fig. 4). It is seen that α increases with increase in Re and H.

It should be noted that at a nonzero angle of incidence a pair of steady vortices lose stability at smaller values of Re than in the case of a symmetric flow. For example, for a cascade with a spacing H = 4, the critical Reynolds numbers are equal to 25 and 62 for $\alpha^- = 26$ and 0^o respectively.

By and large, the index α depends not only on the Reynolds number and the cascade spacing, but also on the angle of incidence of the flow α^-. However, our calculations have shown that this influence is negligibly small. More-

over, comparison of the results of the numerical modeling presented in Figs. 2 and 4 has made it possible to find the dependence of α on $C(\mathrm{Re}, H)$ (see Fig. 5). It turns out that the function $\alpha(C)$ can be approximated in the form

$$\alpha = (1 + C)^{-1.4}. \tag{6}$$

with a root-mean-square deviation of 3%. According to expression (6), the higher the drag of the cascade, the larger the deflections of the flow caused by it.

CONCLUSIONS

The results of the numerical modeling of a steady separation laminar flow of an incompressible viscous fluid around a cascade of circular cylinders have shown that, in a wide range of change in the flow parameters, the refractive index of the cascade is determined by a single parameter — its pressure loss. Only the refractive index determined by formula (1) possesses this property. If α is determined as the ratio between the sines of the angles α^- and α^+, α depends substantially on all three parameters of the flow: the Reynolds number Re, the cascade spacing H, and the angle of attack α^-.

This work was carried out with financial support from the Russian Basic Research Foundation (project 03-01-00015).

NOTATION

C, hydrodynamic drag coefficient of the cascade; C_D, C_f, C_p, drag coefficient of a cylinder, friction drag coefficient, and pressure drag coefficient; D computational region; f and $\langle f \rangle$, right side of the equation for the pressure and its mean; H, cascade spacing; L, number modeling infinity; n and s, normal and tangent to the boundary of the streamlined body; p, pressure; p_1 and p_2, pressure in the cross sections $x = -L$ and $x = L$; Re, Reynolds number; t, time; x, y, Cartesian coordinates; α, refractive index of the cascade; α^- and α^+, angles formed by the normal to the cascade and the velocity vector of the flow upstream and downstream of the row of cylinders; β^- and β^+, angles of inclination of the computational region boundaries upstream and downstream of the cascade; Γ, boundary of the streamlined body; ε, error of the right side of the equation for the pressure; τ, time step of the numerical method; ψ, stream function; ω, vorticity.

REFERENCES

1. M. I. Gurevich, *The Theory of Jets of an Ideal Liquid* [in Russian], Nauka, Moscow (1979).
2. I. E. Idel'chik, *Aerodynamics of Technological Equipment* [in Russian], Mashinostroenie, Moscow (1983).
3. J. W. Elder, Steady flow through non-uniform gauzes of arbitrary shape, *J. Fluid Mech.*, **5**, No. 3, April, 355–368 (1959).
4. P. Roache, *Computational Fluid Dynamics* [Russian translation], Mir, Moscow (1980).
5. O. M. Belotserkovskii, in: *Numerical Modeling in Continuum Mechanics* [in Russian], Nauka, Moscow (1984), pp. 494, 495.
6. A. B. Mazo, Problems of external incompressible fluid flows past bodies at moderate Reynolds numbers, in: *Urgent Problems of Continuum Mechanics* [in Russian], Kazan' (2001), pp. 192–207.
7. A. V. Ermishin and S. A. Isaev (eds.), *Control of Flows past Bodies with Vortex Cells as Applied to Flying Vehicles of Integral Arrangement (Numerical and Physical Modeling)* [in Russian], St. Petersburg (2001), p. 149.
8. M. N. Zakharenkov, Realization of boundary conditions of partial and full slip in solving the Navier–Stokes equations in stream function–vorticity variables, *Zh. Vych. Mat. Mat. Fiz.*, **41**, No. 5, 796–806 (2001).
9. J. Batchelor, in: *An Introduction to Fluid Dynamics* [Russian translation], Mir, Moscow (1973), pp. 326–328, 331.
10. M. Van Dyke, *An Album of Fluid Motion* [Russian translation], Mir, Moscow (1986).

11. S. A. Isaev, A. G. Sudakov, P. A. Baranov, and N. A. Kudryavtsev, Testing of a multiblock algorithm of non-stationary laminar separating flows, *Inzh.-Fiz. Zh.*, **75**, No. 2, 28–35 (2002).
12. P. D. Noymer, Drag on a permeable cylinder in steady flow at moderate Reynolds numbers, *Chem. Eng. Sci.*, **53**, No. 16, 2859–2869 (1998).
13. C. F. Lange, F. Durst, M. Breuer, Wall effects on heat losses from hot-wires, *Int. J. Heat Fluid Flow*, No. 20, 34–47 (1999).